Acta Materia Medica

Research Article

Prognostic value and immune infiltration analyses of cuproptosis-related genes in hepatocellular carcinoma

Graphical abstract

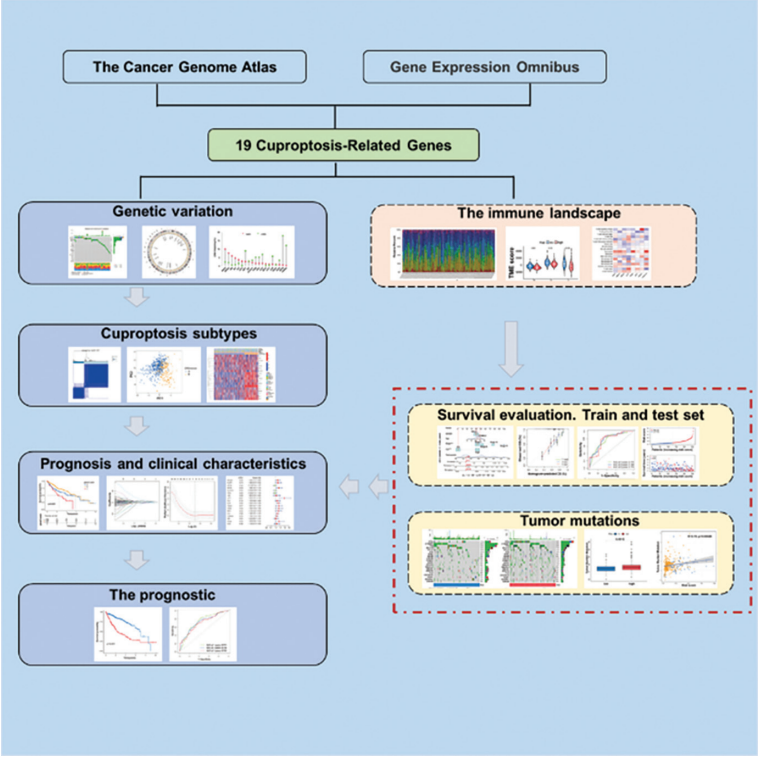

Highlights

- The cuproptosis-related genes (CRGs) exhibited significantly distinct expression patterns in hepatocellular carcinoma (HCC).
- CRGs were positively correlated with majority of infiltrating immune cells.
- The cuproptosis subtypes, gene clusters and survival status demonstrated that CRGs can serve as an independent prognostic indicator for HCC patients.

Authors

Junjie Li, Shuoyi Ma, Yantao Zheng, Mengchen Qin, Hui Jia, Chang Liu, Yunjia Li, Guanghui Deng, Min Cai, Bin Liu and Lei Gao

Correspondence

*raygaolei@smu.edu.cn (L. Gao); nysylb@163.com (B. Liu); simontcm@sohu.com (M. Cai)

In brief

Our findings demonstrated that evaluation of copper-death subtypes provided valuable insights into cancer-related genes, and the copper mortality risk score model played a crucial role in characterizing prognosis and immune infiltration independently of tumor mutational burden.

https://doi.org/10.15212/AMM-2023-0035
386 Acta Materia Medica 2023, Volume 2, Issue 4, p. 386-399

Acta Materia Medica

Research Article

Prognostic value and immune infiltration analyses of cuproptosis-related genes in hepatocellular carcinoma

Junjie Li[a,b,1], Shuoyi Ma[c,1], Yantao Zheng[a,1], Mengchen Qin[b], Hui Jia[b], Chang Liu[b], Yunjia Li[b], Guanghui Deng[b], Min Cai[d,*], Bin Liu[a,*] and Lei Gao[a,b,*]

[a]Zhujiang Hospital, Southern Medical University, Guangzhou, Guangdong 510285, China
[b]School of Traditional Chinese Medicine, Southern Medical University, Guangzhou, Guangdong 510515, China
[c]First People's Hospital, School of Medicine, South China University of Technology, Guangzhou 511436, China
[d]Department of Hepatology, Hainan Provincial Hospital of Chinese Medicine, Haikou, Hainan 570203, China

[1]These authors contributed equally to this work and share first authorship.

***Correspondence:** raygaolei@smu.edu.cn (L. Gao); nysylb@163.com (B. Liu); simontcm@sohu.com (M. Cai)

Received: 5 September 2023; Revised: 24 September 2023; Accepted: 8 October 2023

Published online: 26 October 2023

DOI 10.15212/AMM-2023-0035

ABSTRACT

The role of cuproptosis, a newly discovered form of programmed cell death, remains poorly understood in hepatocellular carcinoma (HCC). This study was aimed at constructing a novel cuproptosis model for analyzing the clinical features, mutation characteristics and immune profile of HCC associated with cuproptosis-related genes (CRG), and to analyze the prognostic value of CRGs in HCC. We comprehensively evaluated HCC datasets containing clinicopathological information from The Cancer Genome Atlas and GEO, on the basis of 19 CRGs. The prognostic value of the cuproptosis-related risk score was established. Our results revealed two clusters associated with cuproptosis. Cluster B exhibited pronounced isolated innate immune cell infiltration and poor prognosis, and significant differences in prognosis and immune infiltration were observed between the groups with high and low cuproptosis risk. High copper mortality risk scores were associated with an elevated tumor mutational burden (TMB) and poor prognosis. Our findings suggest that evaluating copper-death subtypes provides insights into CRGs. Moreover, the copper mortality risk score model aids in characterizing prognosis and immune infiltration independently of the TMB.

Keywords: Cuproptosis, Hepatocellular Carcinoma, Immune infiltration

1. INTRODUCTION

Copper is essential for oxygen reactions, metabolism and iron absorption in eukaryotes [1]. Tsvetkov et al. first identified a novel cell death mode that triggers cell death by directly binding to drive the accumulation of lipid-rich TCA cycle enzymes in mitochondria. The authors observed that increasing copper concentrations induced cell death, thus suggesting copper's toxicity [2]. Under physiological conditions, mitochondria import copper through the carrier family protein SLC25A3 and store it in the matrix, where it is used for cytochrome C oxidase assembly; however, no known protein has been identified as a binder of copper [2, 3]. Copper has been found to promote proliferation, autophagy and lipolysis by binding non-catalytic sites of proteins [4]. In Wilson's disease, *ATP7B* mutation results in excessive copper accumulation, formation of iron-sulfur clusters and decreased the activation of autophagy in hepatocytes [5]. Liver copper deficiency in patients with NAFLD increases steatosis severity, NASH development, and metabolic symptoms [6]. NAFLD forms spontaneously with lipid accumulation in rats deprived of dietary copper [7-9]. In addition, copper deficiency is closely associated with mitochondrial dysfunction and oxidative stress [10]. Decreased liver cellular copper content causes abnormal mitochondrial enlargement, thereby leading to mitochondrial dysfunction [11]. Copper deficiency in the body also leads to abnormal antioxidant function, thus resulting in an aberrant oxidative stress response. Interestingly, disrupted copper metabolism also induces abnormal iron metabolism in the liver and

may potentially be associated with impaired functionality of iron transporters [12, 13]. Thus, cuproptosis has critical regulatory roles in numerous physiological and pathological processes.

HCC is among the top ten most common gross tumors and is the fourth leading cause of tumor-related death [14, 15]. Copper levels have been associated with liver cirrhosis and HCC; moreover, high copper content is associated with poor prognosis and elevated risk of HCC development. Infinite cell proliferation is a crucial hallmark of tumor cells [16-18]. In recent years, induction of programmed cell death in tumor cells has emerged as a potential therapeutic strategy for cancer treatment. The cuproptosis-related gene *FDX1* enhances cuproptosis sensitivity by regulating protein lipoacylation [19]. Copper ions promote cell death through binding fatty acylated components and subsequently lead to abnormal accumulation of fatty acylated proteins, thereby highlighting the beneficial role of copper ions in metabolic diseases. However, the mechanism underlying hepatocyte cuproptosis remains inadequately investigated.

In our study, on the basis of transcriptome data and clinical features, we used an unsupervised clustering algorithm to identify the correlation between cuproptosis-related molecular subtypes and the characteristics of TME cell infiltration. Our findings highlight the major roles of cuproptosis-related molecular subtypes in TME regulation. Furthermore, we used a LASSO Cox regression model to identify genes associated with prognosis, and we constructed a prognostic model for HCC based on the cuproptosis-related risk score (CRRS). To quantify individual patterns of cuproptosis modification in patients with HCC, we developed a nomogram. Finally, we conducted gene cluster analysis and risk score evaluation to assess immune cell infiltration characteristics and immunotherapy sensitivity.

2. MATERIALS AND METHODS

2.1 Downloading and preprocessing of publicly available hepatocellular carcinoma datasets

Transcriptome expression data and survival information for patients with HCC were downloaded from The Cancer Genome Atlas (TCGA) and GEO (http://www.ncbi.nlm.nih.gov/geo/). Patients with HCC with incomplete clinical features were excluded. HCC data from the GEO database and TCGA–Hepatocellular Carcinoma data sets were collected for further analysis. For microarray data, we used the Affy and simplafty software packages to adjust background normalization and perform quantile normalization. HCC gene expression data sets (FPKM values) were downloaded from the Genomic Data Commons (https://portal.gdc.cancer.gov/), and the sva package was used to correct for bulk effects. Similarly, data on somatic mutations were obtained from the TCGA databases and analyzed in R (version 4.1) and the R Bioconductor packages.

2.2 Consensus clustering analysis of 19 cuproptosis-related gene regulators

Initially, 19 CRG regulators were obtained from the published literature and used to construct several CRG modification models. The 19 CRG regulators were *NFE2L2*, *NLRP3*, *ATP7B*, *ATP1A*, *SLC31A1*, *FDX1*, *LIAS*, *LIPT1*, *LIPT2*, *DLD DLAT*, *PDHA1*, *PDHB*, *MTF1*, *GLS*, *CDKN2A*, *DBT*, *GCSH* and *DLST*. Unsupervised clustering analysis was used to classify into two modification modes of CRGs, according to the optimal K value. Patient classification was performed with the ConsensClusterPlus R software package, and the stability of classification was ensured through 1000 cycle calculations. Overall survival (OS) among patients in different clusters was evaluated with the Kaplan-Meier method.

2.3 Identification of differentially expressed genes

We used the limma software package to compare the expression levels of 19 regulators of CRGs between patients with HCC and healthy individuals. The significance threshold for DEGs was set at $|\log FC| > 2$, $P < 0.05$.

2.4 Construction of risk scores associated with cuproptosis

To further evaluate the potential prognostic value and molecular mechanisms of cuproptosis, we performed LASSO Cox regression to analyze the TCGA dataset by using the R glmnet package. The best prognostic biomarkers were screened from among the 19 CRG regulators. Subsequently, risk scores for OS and PFS were calculated separately by using the regression coefficients of the identified prognostic markers of CRGs. Patients were divided into low-risk and high-risk groups according to the median risk score, and their OS values was compared with the R ggsurvplot package in survival analysis. Additionally, we used the nearest-neighbor estimation method to estimate 1-, 3- and 5-year survival rates. The receiver operating characteristic curve was used to evaluate the prognostic value of the survival curve. To further validate the scientific validity of the CRG prognostic model, we used a training set comprising 259 and a test set comprising 258 HCC cases of 517 HCC cases from the TCGA and GSE76427 datasets. On the basis of the significant associations of CRGs with highly malignant and advanced HCC tumors, we constructed a nomogram through uniCox and multiCox analysis to independently analyze the prognostic reliability of the cuproptosis model in HCC and its relationships with clinical factors.

2.5 Comparison of TME cell infiltration

To comprehensively assess the extent of immune cell infiltration in HCC, we performed CIBERSORT analysis to estimate the compositions of immune cell types in HCC samples. We obtained gene sets representing 22 immune cell populations, including activated B cells, CD8 T cells, monocytes, dendritic cells resting T cells,

Acta Materia Medica

macrophages and regulatory T cells. A single sample gene enrichment analysis was used to quantify the relative abundance of different immune cells in TME in each sample species and to assess associations with the CRGs.

2.6 Statistical analysis

T tests were used for the comparison of samples between groups, and one-way ANOVA was used to evaluate differences between three or more groups. Spearman's correlation analysis was used to obtain the correlation coefficient between CRGs and TME immune infiltrating cells. The prognosis was analyzed through uniCox and multiCox regression analysis, and the survival curve was visualized with the Kaplan-Meier method. Chromosome CNV analysis of 19 CRGs was performed with the R RCircos package, and the mutation rates of the 19 CRGs were obtained with the R maftools package. $P < 0.05$ was considered significantly significant, and all data were analyzed in R software 4.1.

3. RESULTS

3.1 Genetic variation in cuproptosis-related genes in HCC

Recent studies have revealed 19 genes associated with CRGs: *NFE2L2*, *NLRP3*, *ATP7B*, *ATP1A*, *SLC31A1*, *FDX1*, *LIAS*, *LIPT1*, *LIPT2*, *DLD DLAT*, *PDHA1*, *PDHB*, *MTF1*, *GLS*, *CDKN2A*, *DBT*, *GCSH* and *DLST*. To investigate the genomic characterization of CRGs in patients with HCC, we evaluated somatic mutations and CNV in 371 HCC samples. The frequency of CRG mutations was approximately 10.24%, thereby indicating a relatively low mutation rate. Among the 19 CRGs, *CDKN2A* (3%) had the highest mutation frequency, and was followed by *NFE2L2* (2%), *NLRP3* (2%), *ATP7A* (1%), *DLD* (1%), *MTF1* (1%) and *DBT* (1%), whereas the remaining CRGs did not exhibit any mutations (Figure 1b). In addition, the CNV analysis results indicated high deletion frequencies for *MTF1*, *DBT*, *SLC31A1*, *PDHB*, *FDX1*, *DLST*, *DLAT*, *GCSH*, *ATP7B* and *CDKN2A* (Figure 1c). Therefore, most CRGs tended to

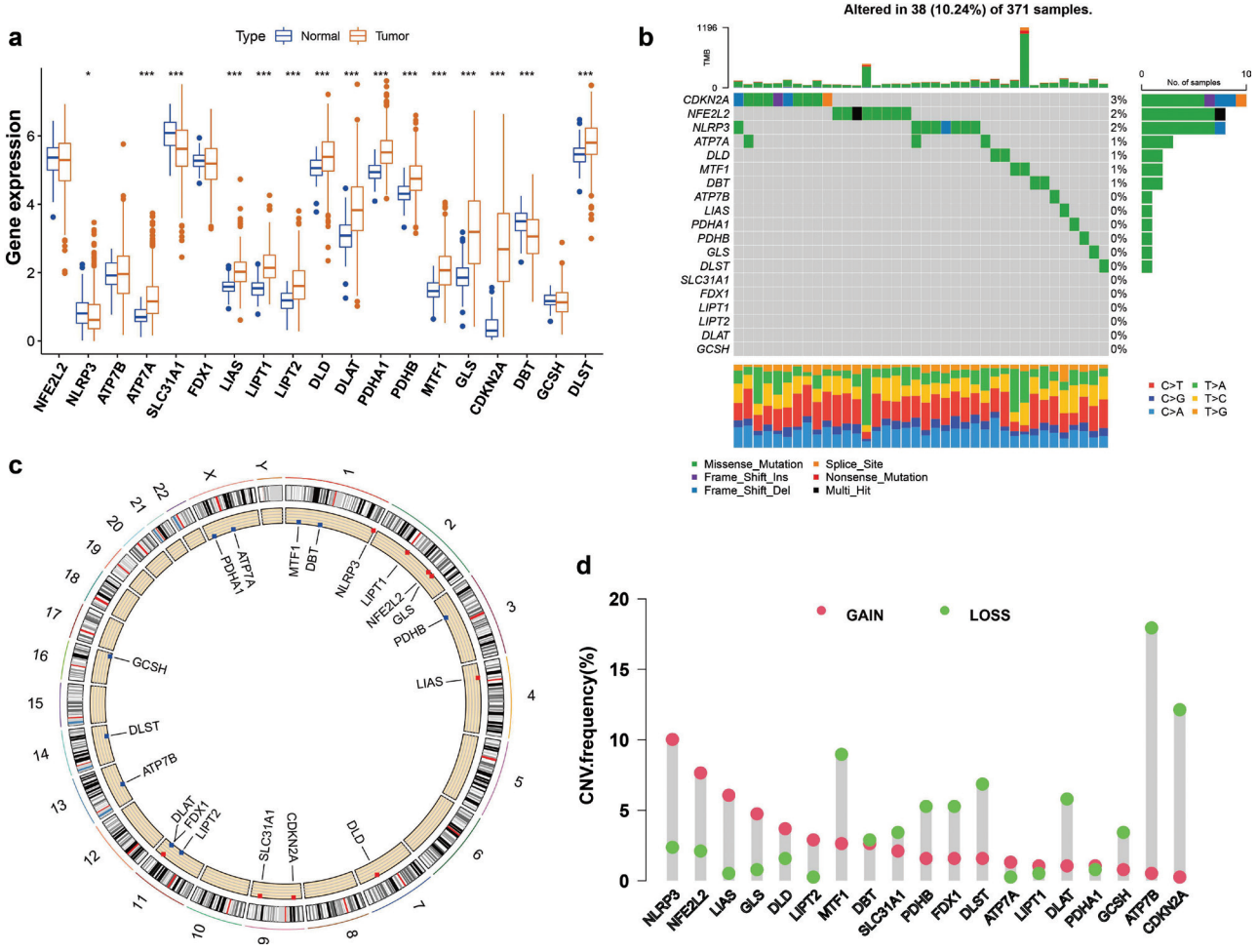

Figure 1 | (a) Differences in the expression of 19 CRGs between patients with HCC and healthy individuals. (b) Mutation frequencies of 19 CRGs in 371 HCC samples, detected with the R maftools package. (c) The CNV frequency of 19 CRGs in liver cancer. (d) Nineteen CRG expression sites on 24 chromosomes. Compared with normal tissues, $*P < 0.05$, $**P < 0.01$, $***P < 0.001$.

be co-deletions rather than co-amplifications with high CNV frequencies. The positions of CNV alterations on chromosomes are depicted in Figure 1d. Furthermore, we evaluated whether abnormal expression of CRGs might be associated with HCC malignancy by comparing mRNA expression levels in HCC and normal tissues, and identified 15 CRGs with significant differential expression patterns (Figure 1a). Moreover, Kaplan-Meier survival curves demonstrated a favorable prognosis associated with the 19 CRG regulators (Figure S1).

3.2 Identification of cuproptosis subtypes in hepatocellular carcinoma

We investigated the clinical significance of CRGs in HCC through univariate Cox and correlation analysis. Nine CRGs (including *LIPT1*, *DLAT* and *GLS*) were significantly associated with negative prognosis in patients with HCC (Figure 2a). To further evaluate the role of CRGs, we used unsupervised clustering analysis to classify the expression levels of CRGs in the HCC cohort with complete survival information (TCGA and GSE76427). This analysis

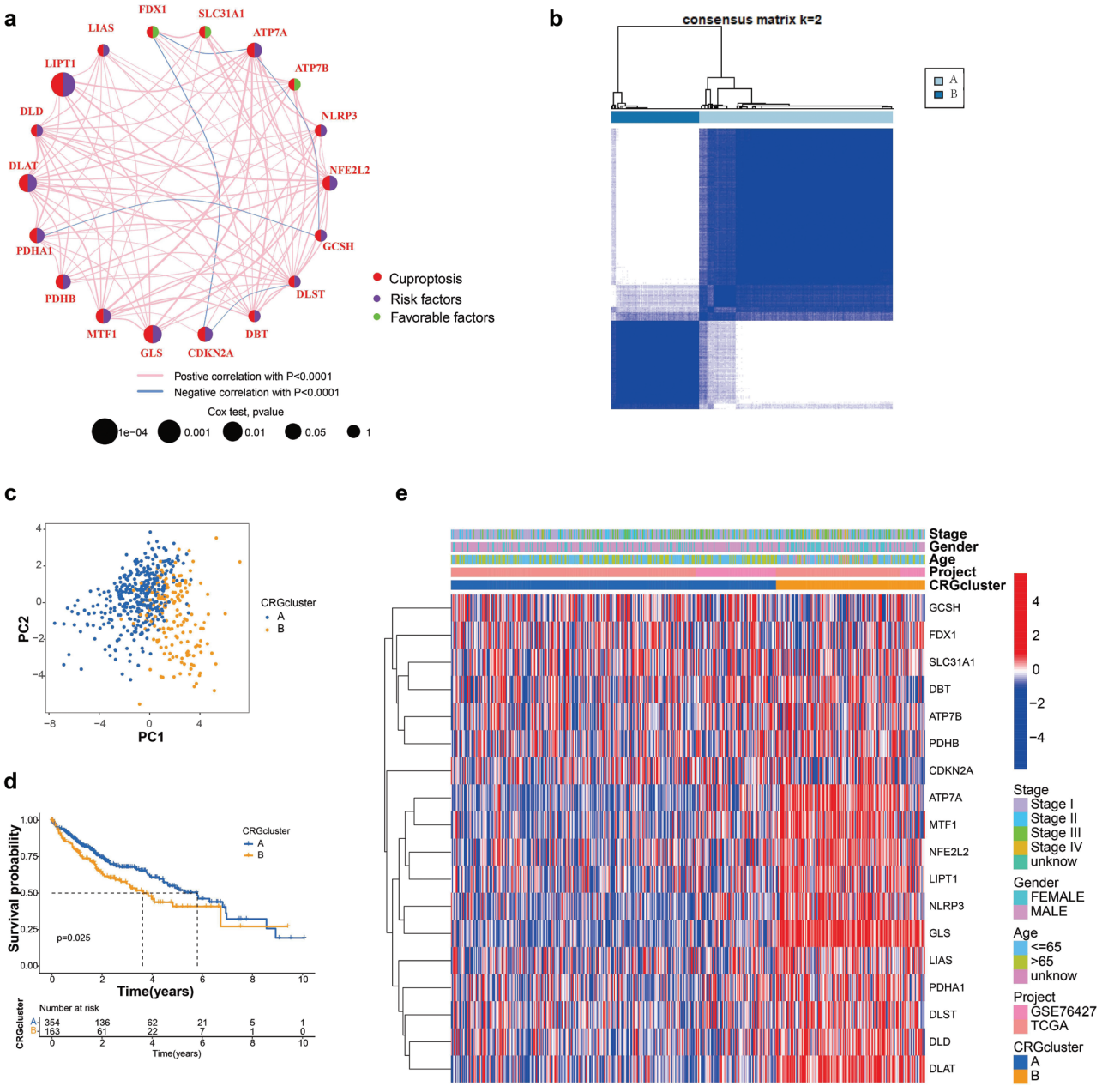

Figure 2 | Construction of cuprotosis subtypes in HCC.
(a) A network of correlations including CRGs in TCGA cohort. (b) Consensus clustering matrix for $k = 2$. (c) Kaplan-Meier curves of OS for two cuprotosis subtypes constructed from 19 CRGs in patients with HCC. (d) Unsupervised clustering analysis of 19 CRGs in HCC.

Acta Materia Medica

identified two distinct regulatory patterns, including 354 cases in CRG-associated cluster A and 163 cases in CRG-associated cluster B (Figure 2b). On the basis of the results of PCA, we divided 371 HCC samples into two distinct subtypes (Figure 2c). In addition, the survival rate of group A was significantly higher than that in group B ($P < 0.05$) (Figure 2d). We illustrated the relationship between clinical factors and gene expression of two different CRG patterns in heat maps (Figure 2e).

3.3 Construction of cuproptosis phenotype-related differentially expressed gene clusters

To further investigate the potential regulatory role of CRG phenotypes, we obtained 4275 DEGs associated with CRGs with the R package Limma and divided them into three clusters according to unsupervised clustering analysis (gene clusters A–C) (Figure 3a), with 206 cases in gene cluster A, 256 cases in gene cluster B and 55 cases in gene cluster C (Figure 3b). Under this clustering algorithm, gene cluster B exhibited a favorable prognosis ($P < 0.001$) (Figure 3d). Interestingly, both gene clusters A and B belonged predominantly to cuproptosis cluster A, whereas patients with gene cluster C belonged to cuproptosis cluster B, which showed poor prognosis (Figure 3c). We observed significant differences in CRG expression among the three gene clusters, in agreement with the anticipated cuproptosis patterns (Figure 3e).

3.4 Prognostic value of cuproptosis-related signatures in HCC

To further investigate the prognostic value of cuproptosis, we developed a prognostic model based on data from 517 patients with HCC with complete survival information in the TCGA and GSE76427 datasets. CRGs with prognostic value were identified through LASSO Cox regression analysis. After establishing a LASSO Cox regression model with lambda minimization, we obtained seven CRGs with cuproptosis-related features and used them to construct a CRRS model (Figure 4a, b). The associations between the expression of seven CRGs and OS was illustrated with a forest plot. The expression levels of *ARF4*, *HMGA1*, *PRKD1*, *TRIB3*, *ZIC2* and *RPPH1* were significantly positively correlated with poor prognosis, whereas that of *IL7R* was significantly negatively correlated with good prognosis (Figure 4c). Differential expression levels of 19 CRGs were observed, whereas *NLRP3*, *ATP7B*, *SLC31A1*, *DBT* and *GCSH* did not show statistically significant differential expression. However, the remaining CRGs had significant effects on prognosis (Figure 4d). The correlations among cuproptosis-subtypes, gene clusters, CRRS and survival status were shown in a Sankey diagram. In the high-CRRS group, a greater proportion of patients experienced death than survived, whereas patients with low CRRS predominated in gene clusters B and C, and the proportion of gene clusters B and C was higher than that of gene cluster A in CRG cluster A (Figure 4e). In addition, the median score of CRG cluster B was significantly lower than that of CRG cluster A. Gene cluster C displayed a higher score than gene clusters A and B, and gene cluster B had the lowest median score (Figure 4f). The low-risk group and high-risk group were divided according to the median risk score. The low-risk group exhibited longer survival time than the high-risk group (Figure 4g), and the area under the receiver operating characteristic curve (AUC) values for 1-year, 3-year and 5-year OS were 0.731, 0.718 and 0.702, respectively (Figure 4h).

3.5 CRGs are an independent prognostic indicator for patients with HCC

On the basis of the significant association of CRGs with highly malignant and advanced HCC tumors, we constructed a nomogram to determine the independent prognostic value of the cuproptosis score in HCC, and its relationship with clinical factors through uniCox and multiCox analysis (Figure 5a). The calibration curve demonstrated excellent agreement between the observed and predicted values of the nomogram (Figure 5b). To further validate the cuproptosis prognosis model, we used 259 of 517 HCC samples as a training set and 258 HCC samples as a test set in survival analysis and Cox regression. The samples were divided into low-risk and high-risk groups according to risk score. Survival analysis revealed that the high-risk group had poorer survival than the low-risk group in training and test set (Figure 5c). Kaplan-Meier curves consistently showed consistent prognostic effects in both datasets. The average AUC values for predicting 1-, 3- and 5-year prognosis in the training set were 0.774, 0.778 and 0.774, respectively, whereas those in the test set were 0.688, 0.658 and 0.638, respectively. (Figure 5d). In two different sets, the training and test set also had the big area under the ROC curve (AUC), thus demonstrating the prognostic efficiency of the risk model. The distribution of disease risk scores and the survival between groups is illustrated in Figure 5e.

3.6 The immune landscape of cuproptosis subtypes

The R package CIBERSORT was used to analyze the proportions of tumor immune infiltrating subsets, and 21 immune cell profiles in HCC samples were constructed (Figure 6a). A heat map was generated to illustrate the correlations among these 21 immune cell types (Figure 6b). We investigated TME cell infiltration on the basis of two constructed clusters. CD4 T cells, dendritic cells, eosinophils, natural killer cells, natural killer T cells, regulatory T cells, THC, TH1, TH2 and TH17 T cells were more significantly clustered in cluster B (Figure 6c). In addition, a tumor-associated stromal score and an immune score representing the level of immune infiltration were obtained with the ESTIMATE algorithm. These scores were combined to generate an index called the "estimated score" to infer tumor purity. The estimated scores, stromal scores and immune scores were lower in the high-risk group than the low-risk group (Figure 7a).

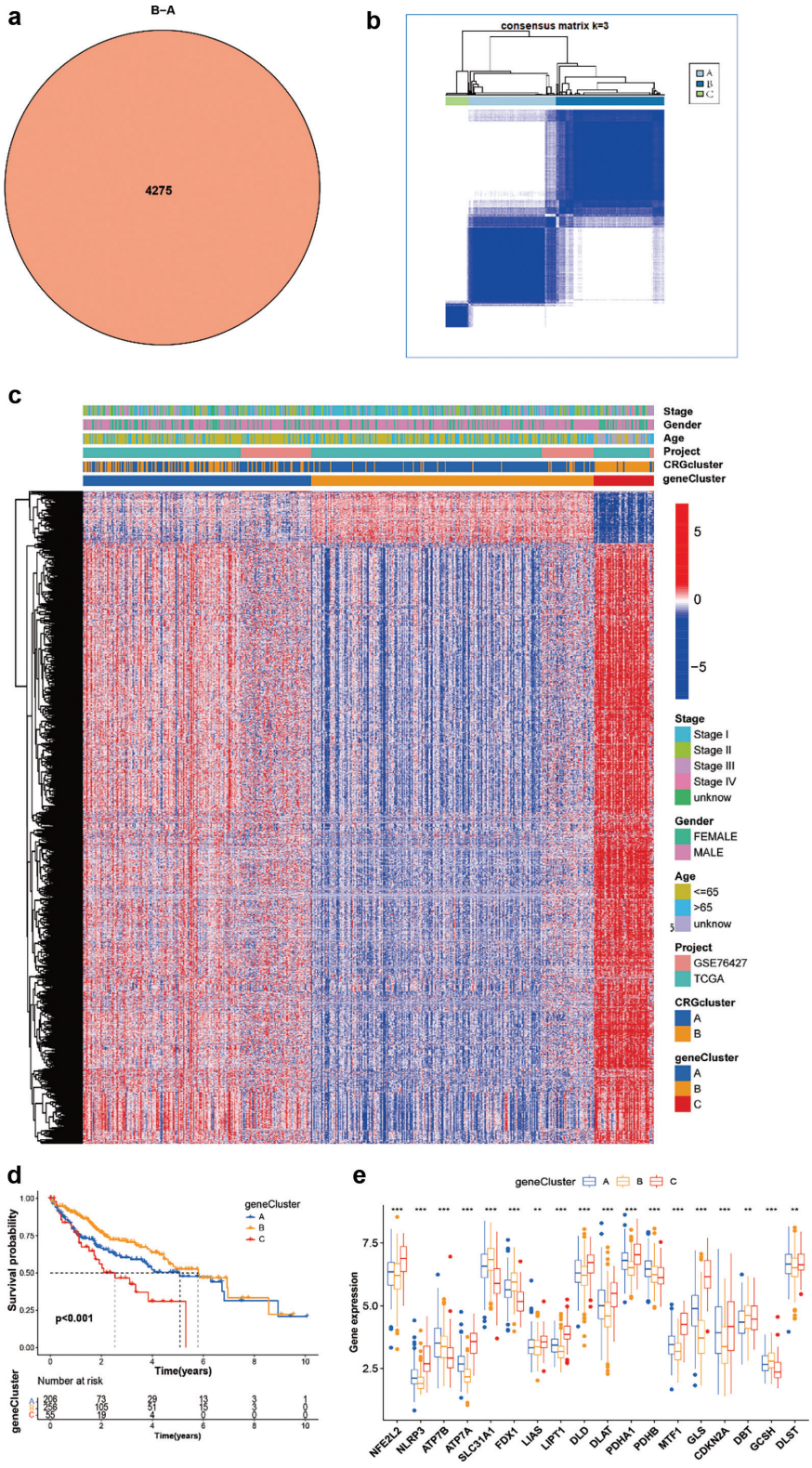

Figure 3 | Prognosis and clinical characteristics of three cuproptosis gene clusters from patients with HCC.
(a) Venn diagram indicating genes shared by two cuproptosis subtypes. (b) Consensus matrix heat maps for three gene clusters, obtained with the R ConsensClusterPlus package. (c) Heat maps of clinical characteristics of three cuproptosis gene clusters. (d) Kaplan-Meier survival curve of the survival probabilities of patients with three gene clusters. (e) Expression of 19 CRGs in three gene clusters.

Acta
Materia
Medica

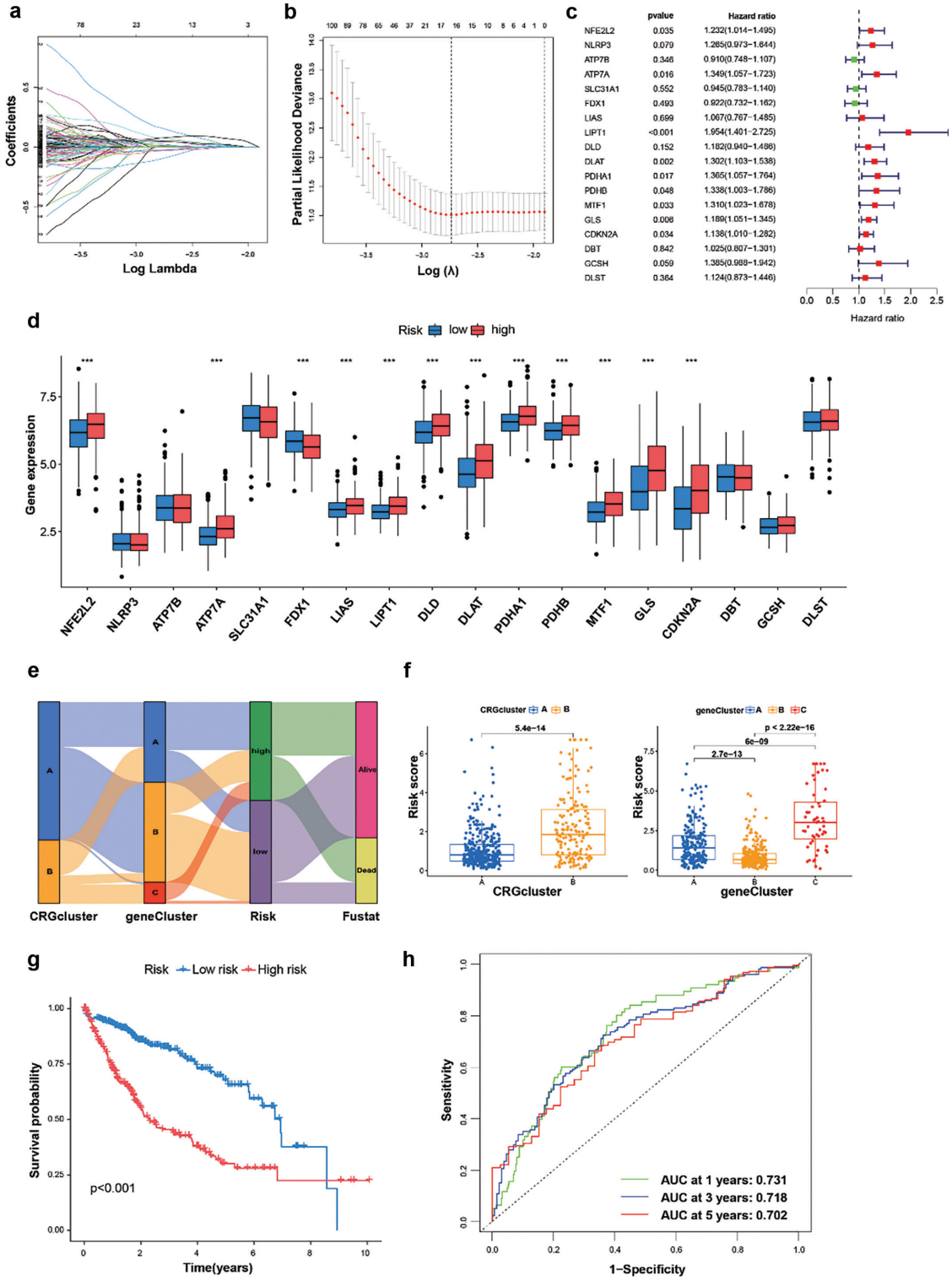

Figure 4 | Determination of CRGs for prediction of HCC prognosis.
(a, b) LASSO regression analysis performed in the R glmnet package on 19 CRGs, showing the distribution of LASSO coefficients and partial likelihood deviance. (c) Forest plots of correlations between 19 CRGs and survival. (d) Expression of 19 CRGs in the high-risk and low-risk groups. (e) Sankey diagram showing the relationships among CRG clustering, gene clustering, risk coefficient and survival state. (f) Kruskal-Wallis test analysis of differences in risk scores between two CRG clusters and three gene clusters. (g) Kaplan-Meier curves showing survival in the high-risk and low-risk groups. (h) ROC analysis of CRGs and survival state.

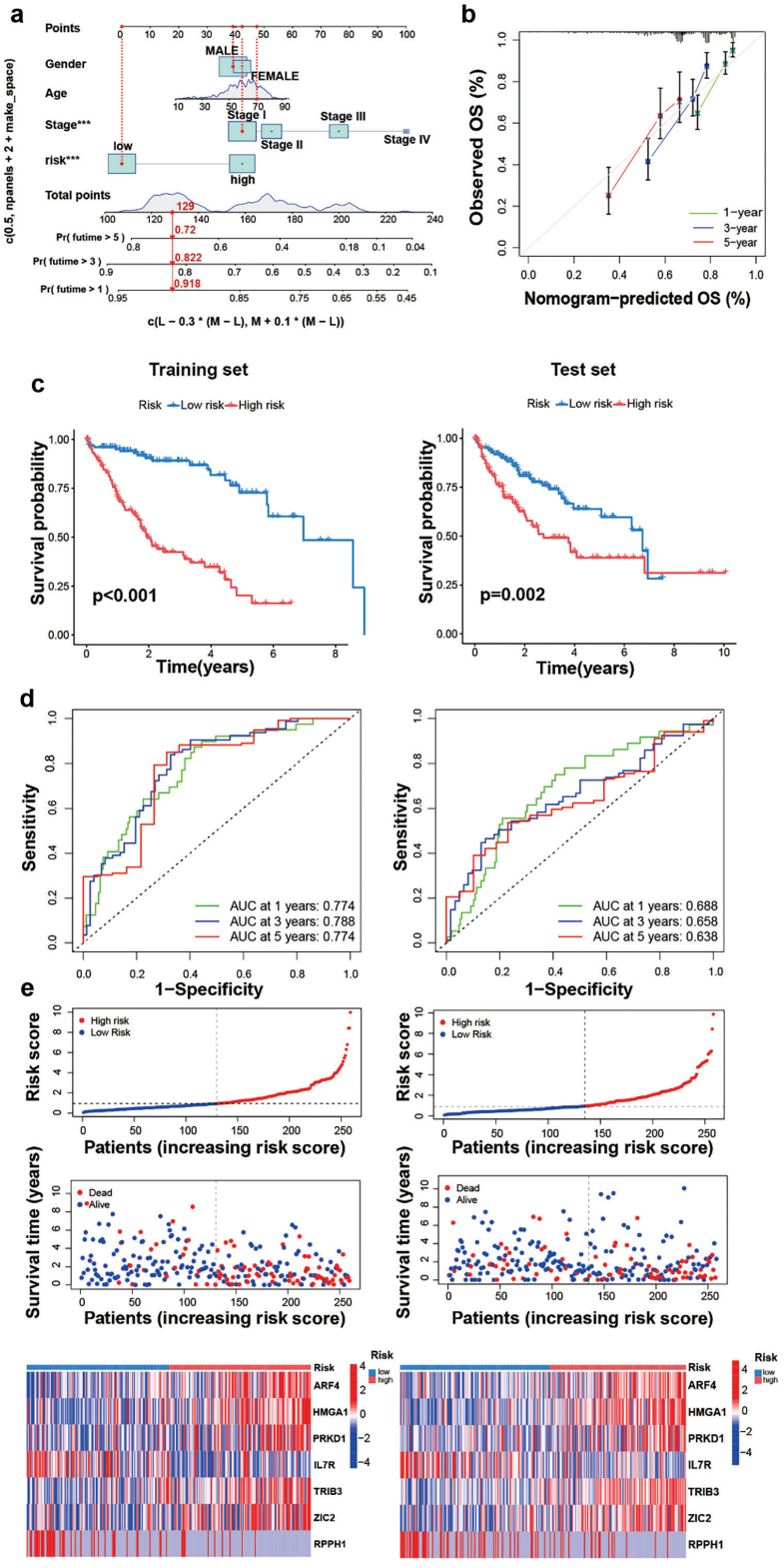

Figure 5 | Survival evaluation, on the basis of CRGs in the training and test set.
(a, b) Comprehensive nomograms and calibration maps for predicting 1-, 3- and 5-year survival of patients with HCC. (c) Kaplan-Meier survival curves showing survival rates with high or low risk scores in the training and test groups. (d, e) ROC curves, 1-, 3- and 5-year survival profiles and heat maps of prognostic molecules for the training and testing sets.

Acta
Materia
Medica

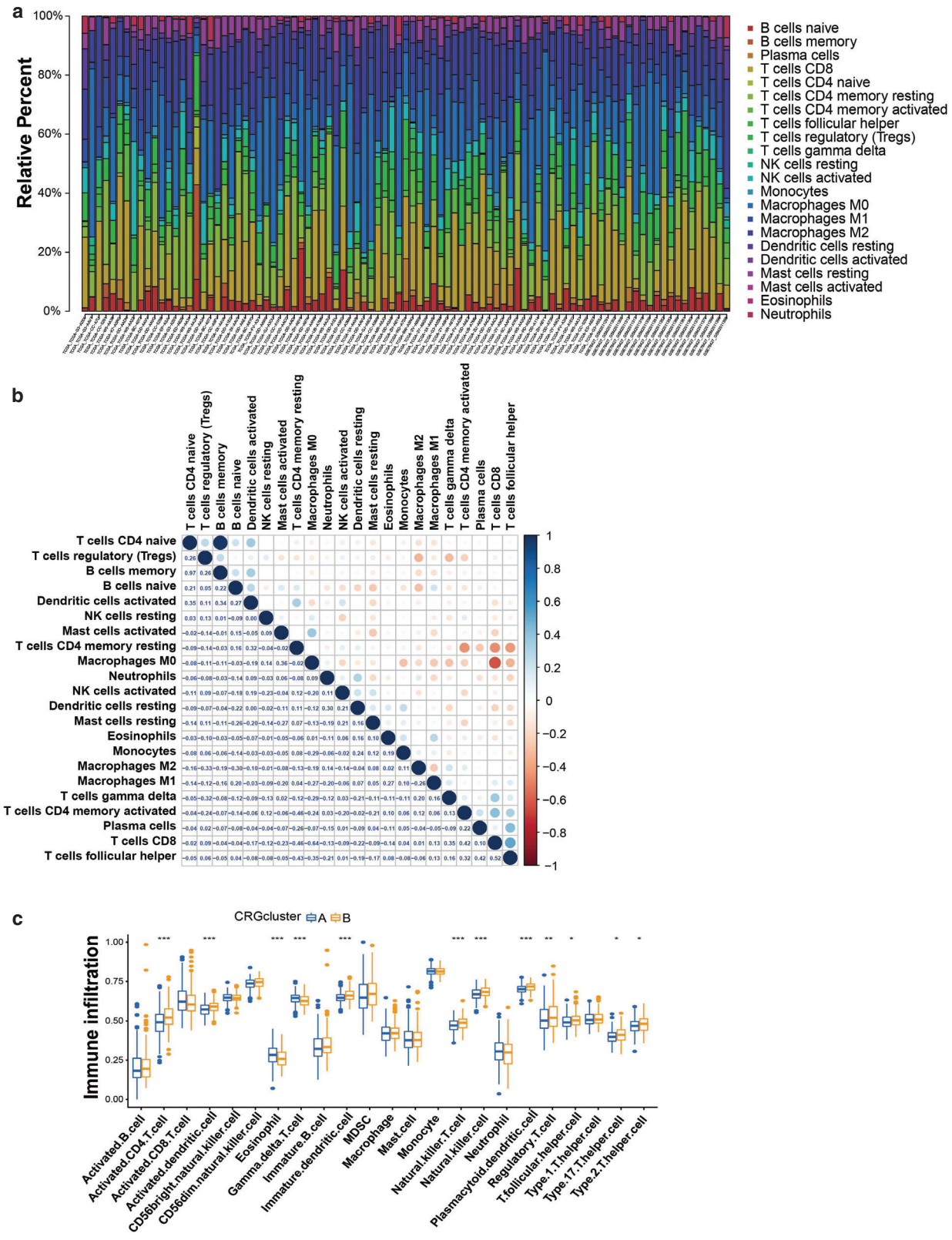

Figure 6 | Immune landscape of cuproptosis subtypes.
(a) The relative proportions of 21 immune cell types in HCC. (b) Correlation analysis among 21 types of immune cells. (c) Expression abundance of different TME infiltrating cells in two CRG clusters.

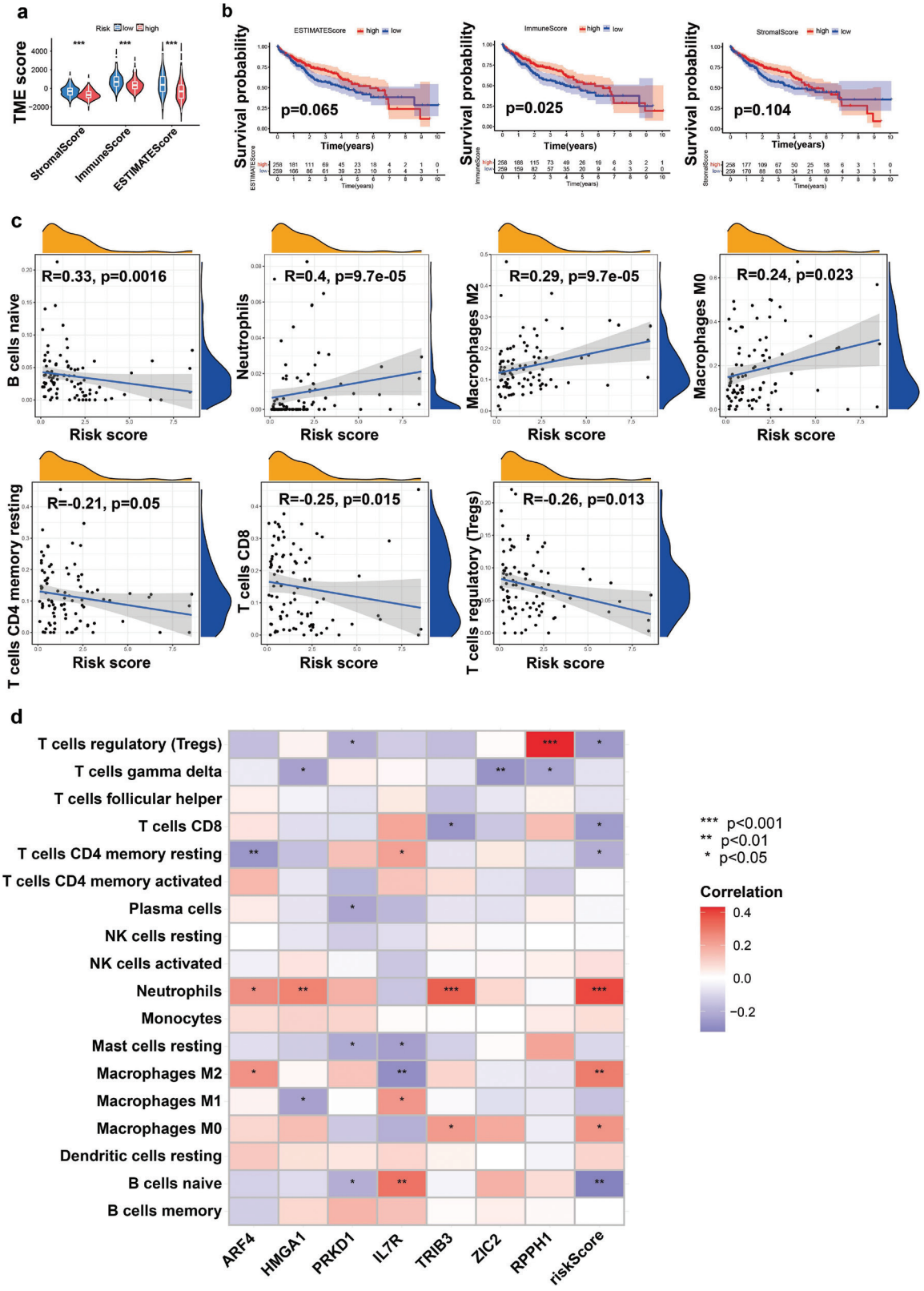

Figure 7 | (a) Differences in TME score between high and low risk-score group. (b) Kaplan–Meier survival analysis for patients in the TME score. (c) Scatterplots showing the correlation between CRGs and TMB. (d) Spearman analysis of the correlation between CRGs and ICI abundance.

Acta
Materia
Medica

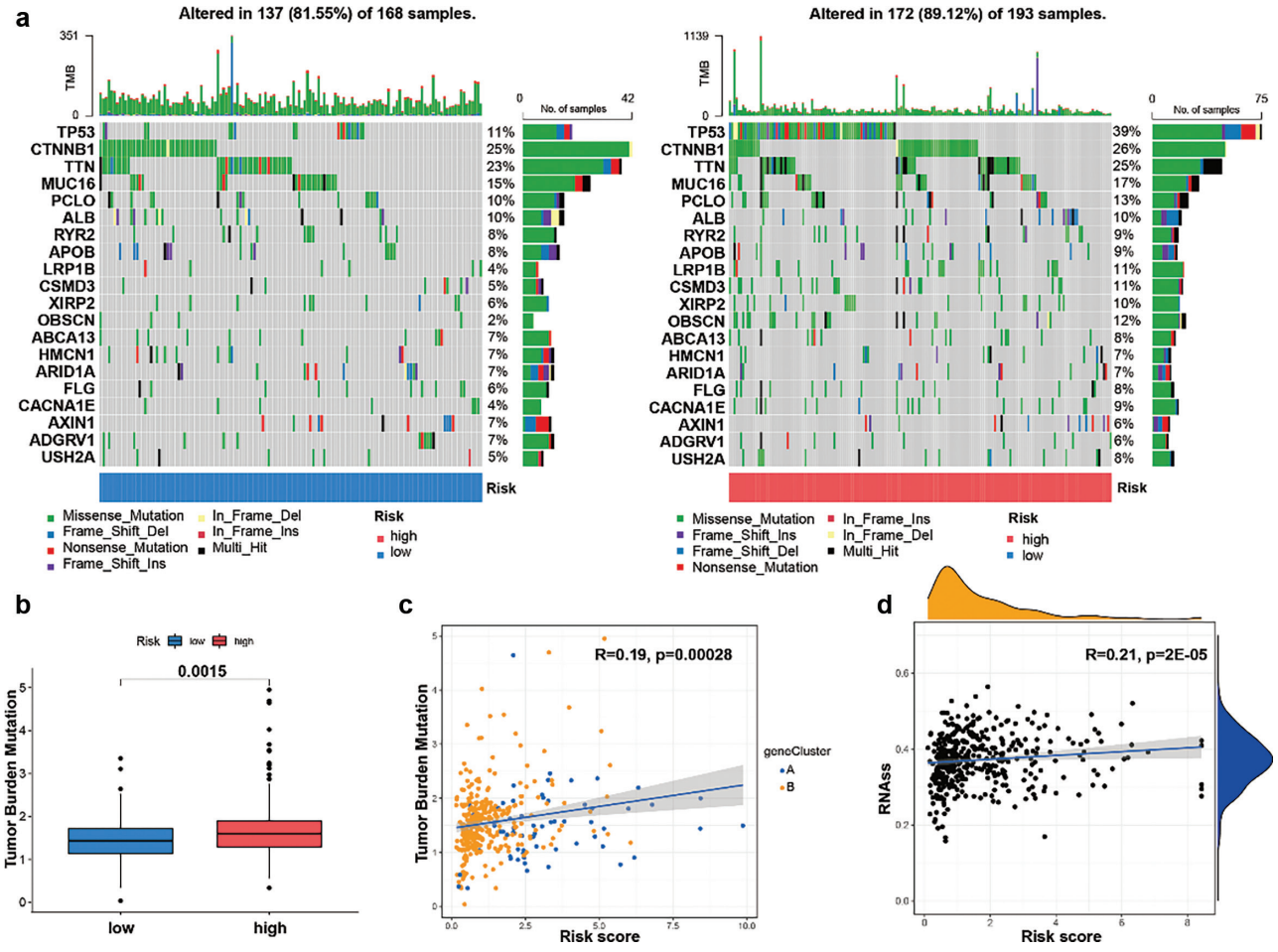

Figure 8 | Characteristics of CRG modification in tumor somatic mutation.
(a) Waterfall-diagram visualization of tumor somatic mutations in low- and high-risk groups. (b) Statistical differences in TMB between the high- and low-risk groups, according to the Wilcoxon Rank Sum test. (c) Scatter plot showing a significant positive correlation between risk score and TMB. (d) Scatter plots showing a significant positive correlation between risk score and RNAs.

However, these scores did not demonstrate any significant correlation with patient clinical characteristics (sex, age or stage) (Figure S2). We hypothesized that CRGs might influence tumorigenesis in some other way; therefore, we investigated the correlation between CRGs and inflammatory infiltration. Neutrophils, and M0 and M2 macrophages, were significantly positively correlated with the risk score, whereas B cells, CD4 T cells, CD8 T cells and regulatory T cells displayed a negative correlation (Figure 7c). We subsequently explored the correlations of immune cells and CRGs with favorable prognosis, and generated a heat map (Figure 7d). The findings unveiled the involvement of CRGs in the regulation of immune infiltration.

3.7 Characteristics of the cuproptosis score with respect to tumor mutations

Subsequently, we used the maftools software package to comprehensively analyze the distribution of somatic mutations between CRGs in the high-risk and low-risk groups in patients with HCC in TCGA (Figures 8a, b). To further explore somatic mutations among patients with HCC in the high-risk and low-risk groups, we used the R maftools package for analysis. The mutation rate of the CTNNB1 gene was higher in the high-risk group than the low-risk group (25% vs 26%, respectively). Additionally, TMB and RNA quantitative analysis confirmed that CRGs in the high-risk group were significantly positively correlated with TMB and RNA levels (Figure 8c, d).

4. DISCUSSION

Unrestrained proliferation is a hallmark of tumor cells, which evade growth inhibition by resisting cell death and evading immune-mediated killing. Induction of programmed cell death is an effective strategy in tumor therapy [20]. Studies have shown that programmed cell death has several modes, including apoptosis,

neuroapoptosis, cell necrosis and ferroptosis. Excess copper induces cell death, similarly to iron [14]. Recently, the term cuproplasia has been proposed to describe the phenotypic manifestation of this particular tumor type, characterized by copper-dependent cellular proliferation [21]. However, the exact mechanism remains unclear [22]. Tsvetkov et al. have found that cell death is induced when copper is loaded on elesclomol (a copper ionophore) [22]. Those findings suggest a new potential therapeutic approach for treating tumors. In our study, we explored the expression profiles of 19 CRGs in HCC tissues. The reliability of clustering was demonstrated through PCA by construction of two cuproptosis clusters with significantly different immune infiltration and FRG features. Cuproptosis cluster B exhibited high immune cell infiltration but interestingly contained many innate immune cells, such as dendritic cells, eosinophils, natural killer cells, natural killer T cells and regulatory T cells. Copper is essential for the development and maintenance of immune function. Several findings have suggested that copper deficiency disrupts immune function, and an increased copper ion content inhibits the antigen presentation from dendritic cells to T cells, and the proliferation of T cells. Increasing copper concentrations have been found to promote the killing effect of macrophages through the Fenton reaction, thereby producing ROS [23]. By inhibiting the phosphorylation of *STAT3* and *EGFR*, copper chelators facilitate the ubiquitination of *PD-L1* and significantly enhance the ability of CD8 T cells and natural killer cells to suppress tumor growth [24]. In contrast, CRG-based risk models have revealed significant correlations among neutrophils, macrophages, B cells, CD4 T cells and CD8 T cells. Clinical evidence has demonstrated significantly higher serum copper levels among patients with HCC than those with chronic hepatitis, and the copper concentration is closely associated with both the incidence and progression of HCC [25]. In addition, the expression of mammalian ferredoxin 1 (FDX1) is regulated by adrenomedullin, which effectively inhibits copper-induced cell death and promotes tumor growth. Moreover, the critical role of copper-mediated cell death in tumor progression and chemotherapy resistance has been demonstrated, on the basis of the enhancement of sunitinib resistance observed in clear cell renal cell carcinoma. Therefore, cuproptosis is closely associated with tumors and affects tumor development through the tumor immune microenvironment. However, further validation is required to substantiate the role of CRGs in regulating therapeutic interventions and tumor immunity [26].

We identified three clusters of DEGs associated with copper-induced mortality, according to analysis in the R package. The prognostic analysis of these DEG clusters was consistent with the survival probabilities of the CRG cluster. We demonstrated the roles of alterations in cuproptosis in the prognostication and diagnosis of HCC. Therefore, on the basis of prognostic characteristics, we explored the prognostic and clinical value of the copper mortality score in HCC. Studies have demonstrated that CRG signatures have substantial prognostic value in assessing survival outcomes among patients with HCC. In addition, the prognostic ability of the model was evaluated with training and test datasets, and the two datasets had supported a good prognostic results. Our results also highlighted that CRGs may serve as a valuable prognostic indicator for HCC.

However, further improvements are required. The analysis of the cuproptosis prognostic model in this study was based on public databases. Because of the limited availability of clinical samples, some deviations might exist in the clinical data. In addition, although we observed interactions between CRGs and immune cells, the mechanism underlying these phenomena remains unclear and must be further verified through in vitro and in vivo experiments.

Nevertheless, our study demonstrated that the CRG model exhibited robust prognostic features for HCC and was associated with immune infiltration. Therefore, this model has potential as an indicator for predicting HCC survival and prognosis.

ABBREVIATIONS

TCGA, The Cancer Genome Atlas; CRG, Copper-related gene; OS, Overall survival; TMB, Tumor mutational burden.

ACKNOWLEDGEMENTS

This study was financially supported by the National Natural Science Foundation of China (82260926, 82004105 and 82000595), Guangdong Basic and Applied Basic Research Foundation (2018B030306012, 2023A1515010383), the Young Elite Scientists Sponsorship Program by CACM (2021-QNRC2-B28) and the Hainan Province Science and Technology Special Fund (ZDKJ2021034).

CONFLICT OF INTEREST

The authors declare that this research was conducted in the absence of any commercial or financial relationships that could be construed as a potential conflict of interest.

REFERENCES

[1] Robinson NJ, Winge DR: Copper Metallochaperones. *Annual Review of Biochemistry* 2010, 79:537–562.

[2] Tsvetkov P, Coy S, Petrova B, Dreishpoon M, Verma A, Abdusamad M, et al.: Copper Induces Cell Death by Targeting Lipoylated TCA Cycle Proteins. *Science* 2022, 375:1254–1261.

[3] Zhu X, Boulet A, Buckley KM, Phillips CB, Gammon MG, Oldfather LE, et al.: Mitochondrial Copper and Phosphate Transporter Specificity was Defined Early in the Evolution of Eukaryotes. *Elife* 2021, 10:e64690.

[4] Semrau JD, DiSpirito AA, Yoon S: Methanotrophs and Copper. *FEMS Microbiology Reviews* 2010, 34:496–531.

[5] Polishchuk EV, Merolla A, Lichtmannegger J, Romano A, Indrieri A, Ilyechova EY, et al.: Activation of Autophagy, Observed in Liver Tissues from Patients with Wilson Disease and from ATP7B-Deficient Animals, Protects Hepatocytes

from Copper-Induced Apoptosis. *Gastroenterology* 2019, 156:1173–1189.e1175.

[6] Aigner E, Theurl I, Haufe H, Seifert M, Hohla F, Scharinger L, et al.: Copper Availability Contributes to Iron Perturbations in Human Nonalcoholic Fatty Liver Disease. *Gastroenterology* 2008, 135:680–688.

[7] Aigner E, Strasser M, Haufe H, Sonnweber T, Hohla F, Stadlmayr A, et al.: A Role for Low Hepatic Copper Concentrations in Nonalcoholic Fatty Liver Disease. *The American Journal of Gastroenterology* 2010, 105:1978–1985.

[8] Lan Y, Wu S, Wang Y, Chen S, Liao W, Zhang X, et al.: Association between Blood Copper and Nonalcoholic Fatty Liver Disease According to Sex. *Clinical Nutrition* 2021, 40:2045–2052.

[9] Antonucci L, Porcu C, Iannucci G, Balsano C, Barbaro B: Non-Alcoholic Fatty Liver Disease and Nutritional Implications: Special Focus on Copper. *Nutrients* 2017, 9:1137.

[10] Begriche K, Massart J, Robin MA, Bonnet F, Fromenty B: Mitochondrial Adaptations and Dysfunctions in Nonalcoholic Fatty Liver Disease. *Hepatology* 2013, 58:1497–1507.

[11] Chimienti G, Orlando A, Russo F, D'Attoma B, Aragno M, Aimaretti E, et al.: The Mitochondrial Trigger in an Animal Model of Nonalcoholic Fatty Liver Disease. *Genes (Basel)* 2021, 12:1439.

[12] Tallino S, Duffy M, Ralle M, Cortés MP, Latorre M, Burkhead JL: Nutrigenomics Analysis Reveals that Copper Deficiency and Dietary Sucrose Up-Regulate Inflammation, Fibrosis and Lipogenic Pathways in a Mature Rat Model of Nonalcoholic Fatty Liver Disease. *The Journal of Nutritional Biochemistry* 2015, 26:996–1006.

[13] Song M, Vos MB, McClain CJ: Copper-Fructose Interactions: A Novel Mechanism in the Pathogenesis of NAFLD. *Nutrients* 2018, 10:1815.

[14] Chidambaranathan-Reghupaty S, Fisher PB, Sarkar D: Hepatocellular Carcinoma (HCC): Epidemiology, Etiology and Molecular Classification. *Advances in Cancer Research* 2021, 149:1–61.

[15] Llovet JM, Kelley RK, Villanueva A, Singal AG, Pikarsky E, Roayaie S, et al.: Hepatocellular Carcinoma. *Nature Reviews. Disease Primers* 2021, 7:6.

[16] Fang AP, Chen PY, Wang XY, Liu ZY, Zhang DM, Luo Y, et al.: Serum Copper and Zinc Levels at Diagnosis and Hepatocellular Carcinoma Survival in the Guangdong Liver Cancer Cohort. *International Journal of Cancer* 2019, 144:2823–2832.

[17] Hanahan D, Weinberg RA: Hallmarks of Cancer: The Next Generation. *Cell* 2011, 144:646–674.

[18] Qin X, Ma D, Tan YX, Wang HY, Cai Z: The Role of Necroptosis in Cancer: A Double-Edged Sword? *Biochimica et Biophysica Acta. Reviews on Cancer* 2019, 1871:259–266.

[19] Tsvetkov P, Detappe A, Cai K, Keys HR, Brune Z, Ying W, et al.: Mitochondrial Metabolism Promotes Adaptation to Proteotoxic Stress. *Nature Chemical Biology* 2019, 15:681–689.

[20] Yamaguchi K, Yokoi K, Umezawa M, Tsuchiya K, Yamada Y, Aoki S: Design, Synthesis, and Anticancer Activity of Triptycene-Peptide Hybrids that Induce Paraptotic Cell Death in Cancer Cells. *Bioconjugate Chemistry*. 2022, 33:691–717.

[21] Ge EJ, Bush AI, Casini A, Cobine PA, Cross JR, DeNicola GM, et al.: Connecting Copper and Cancer: From Transition Metal Signalling to Metalloplasia. *Nature Reviews. Cancer* 2022, 22:102–113.

[22] Bock FJ, Tait SWG: Mitochondria as Multifaceted Regulators of Cell Death. *Nature Reviews. Molecular Cell Biology* 2020, 21:85–100.

[23] Schuhladen K, Stich L, Schmidt J, Steinkasserer A, Boccaccini AR, Zinser E: Cu, Zn Doped Borate Bioactive Glasses: Antibacterial Efficacy and Dose-Dependent In Vitro Modulation of Murine Dendritic Cells. *Biomaterials Science* 2020, 8:2143–2155.

[24] Voli F, Valli E, Lerra L, Kimpton K, Saletta F, Giorgi FM, et al.: Intratumoral Copper Modulates PD-L1 Expression and Influences Tumor Immune Evasion. *Cancer Research* 2020, 80:4129–4144.

[25] Ke C, Dai S, Xu F, Yuan J, Fan S, Chen Y, et al.: Cuproptosis Regulatory Genes Greatly Contribute to Clinical Assessments of Hepatocellular Carcinoma. *BMC Cancer* 2023, 23:25.

[26] Wang X, Jia JH, Zhang M, Meng QS, Yan BW, Ma ZY, et al.: Adrenomedullin/FOXO3 Enhances Sunitinib Resistance in Clear Cell Renal Cell Carcinoma by Inhibiting FDX1 Expression and Cuproptosis. *FASEB Journal* 2023, 37:e23143.